



OPEN

SUBJECT AREAS:

SENSORS AND  
BIOSENSORS

METAL-ORGANIC FRAMEWORKS

Received  
23 May 2014Accepted  
11 August 2014Published  
1 September 2014

Correspondence and  
requests for materials  
should be addressed to  
M.K. (mkimura@  
shinshu-u.ac.jp)

# Detection of Volatile Organic Compounds by Weight-Detectable Sensors coated with Metal-Organic Frameworks

Hiroki Yamagiwa<sup>1</sup>, Seiko Sato<sup>1</sup>, Tadashi Fukawa<sup>1</sup>, Tsuyoshi Ikehara<sup>2</sup>, Ryutaro Maeda<sup>2</sup>, Takashi Mihara<sup>3</sup> & Mutsumi Kimura<sup>1</sup>

<sup>1</sup>Faculty of Textile Science and Technology, Shinshu University, Ueda 386-8567, Japan, <sup>2</sup>National Institute of Advanced Industrial Science and Technology (AIST), 1-2 Namiki, Tsukuba 305-8564, Japan, <sup>3</sup>Future Creation Laboratory, Olympus Corporation, Tokyo 192-8512, Japan.

**Detection of volatile organic compounds (VOCs) using weight-detectable quartz microbalance and silicon-based microcantilever sensors coated with crystalline metal-organic framework (MOF) thin films is described in this paper. The thin films of two MOFs were grown from COOH-terminated self-assembled monolayers onto the gold electrodes of sensor platforms. The MOF layers worked as the effective concentrators of VOC gases, and the adsorption/desorption processes of the VOCs could be monitored by the frequency changes of weight-detectable sensors. Moreover, the MOF layers provided VOC sensing selectivity to the weight-detectable sensors through the size-selective adsorption of the VOCs within the regulated nanospace of the MOFs.**

On-site and real-time detection of VOCs is a critical and challenging issue for environmental and health monitoring. VOC detection systems have been developed as electronic nose systems composed of an array of several different sensors and a pattern recognition system<sup>1–3</sup>. Electronic gas sensors within the electronic nose systems are capable of converting chemical information into an output signal, and each sensor in the array can generate different signals in response to the concentration and specific interaction with the target VOCs<sup>4</sup>. Gas sensors, which are based on the chemical sensitivity of metal oxide semiconductors (MOS), are commercially readily available<sup>5</sup>. Although MOS sensors have been widely used to create arrays for VOC sensing, these sensors require heating the sensing layer at 200–400°C for their operation. Electromechanical devices such as quartz crystal microbalances (QCMs) and microcantilevers have been used in chemical sensing using various sensing materials to overcome these disadvantages of MOS sensors<sup>6,7</sup>. These devices detect analytes by sensing small changes in the frequency of a resonant vibration as a result of weight changes on a nanogram level. The sensing materials on electromechanical devices accumulate the target analytes and transduce the weight changes into the frequency shifts of the sensors. We previously demonstrated the detection of VOCs by using the QCM and microcantilever sensor arrays deposited with polymers and organic-inorganic hybrid materials<sup>8–11</sup>. The large surface area and porosity of porous titanium oxide (TiO<sub>2</sub>) films enhanced their sensitivity to VOC gases<sup>11</sup>. Covering the TiO<sub>2</sub> surface with polymer layers improved the repeatability and responsibility for the VOC sensing compared to the sensors with only polymer layers. The tunability and structural diversity of organic-inorganic hybrid materials enables for the creation of a pattern recognition library of chemical sensor arrays.

Special attention has been paid to MOFs due to their potential applications such as gas storage/purification, catalysis, and chemosensors based on their tunable nanoporosity and high surface area<sup>12–17</sup>. The connection of metal ions or clusters with multitopic organic linkers creates a regulated nanospace within the extended crystalline structures. The guest molecules can be incorporated into the nanospace of MOFs through their molecular sieving effects,  $\pi$ - $\pi$  interaction, hydrogen bonding, and electrostatic interactions, etc. The nanospace in MOFs can recognize the size and shape of guest molecules, and their high surface-areas make them promising candidates for a variety of sensing applications. Several groups have reported on chemical detections of small guest molecules though the integration of MOFs into devices such as QCM, surface plasmon resonance spectroscopy, surface acoustic wave devices, and microcantilevers<sup>18–20</sup>. Biemmi et al. demonstrated the direct growth of MOFs on gold



electrodes on QCMs to evaluate the water-sorption properties of MOF thin films<sup>21</sup>. Allendorf et al. succeeded in the chemical detection of gases by monitoring the stress generation between a microcantilever and a MOF thin film in response to the molecular adsorption within crystalline MOFs<sup>22</sup>. MOF thin films deposited onto these sensor platforms are an effective concentrator for low-concentration analytes, and also provide the selectivity for analyte species<sup>23</sup>.

We discussed the highly sensitive and selective detection of VOCs through the integration of MOF thin films with weight detectable sensor platforms in this paper. Thin films of two MOFs [Cu<sub>3</sub>(BTC)<sub>2</sub>(H<sub>2</sub>O)<sub>3</sub>]·xH<sub>2</sub>O (BTC = 1,3,5-benzenetricarboxylate)<sup>24</sup> and [Zn<sub>4</sub>O(BDC)<sub>3</sub>] (BDC = 1,4-benzenedicarboxylate)<sup>25</sup> were grown from COOH-terminated self-assembled monolayers (SAM) onto the gold electrodes of QCMs or silicon microcantilevers. The structures and morphologies of the resulting MOF films were probed using grazing incidence X-ray diffraction (GIXRD), infrared reflection absorption spectroscopy (FT-IR-RAS), and scanning electron microscopes (SEM) images. The stiff MOF architectures could transduce the weight changes of the VOCs adsorption/desorption into the frequency changes of the weight-detectable sensors, and the adsorption dynamics of the VOCs into the MOFs were monitored directly through the frequency changes of the sensors. The structural difference between Cu<sub>3</sub>(BTC)<sub>2</sub> and Zn<sub>4</sub>O(BDC)<sub>3</sub> affected the responsibility and selectivity of the VOC sensing.

## Results

VOC sensors have been developed by modifying the surface of sensor platforms with various kinds of sensing materials, and these sensors can be used for monitoring dynamic processes such as chemisorption, reaction, and intermolecular interactions<sup>1–3</sup>. When the target molecules are captured within the sensing layers on the weight-detectable devices, the sorption amounts can be monitored based on their frequency changes. The VOC sorption and desorption processes within the porous MOFs in this study were monitored by the frequency changes of the surface-modified weight detectable sensors. MOFs can be grown as crystalline thin films on solid surfaces through two self-assembling processes<sup>26–31</sup>. Shekhah et al. reported on the step-by-step synthesis of MOF thin films on a SAM by using two solutions of metal ions and ligands<sup>26</sup>. Bein et al. demonstrated the oriented crystal growth of Cu<sub>3</sub>(BTC)<sub>2</sub> on different functionalized SAMs using crystallization solutions containing colloidal or molecular building blocks of Cu<sub>3</sub>(BTC)<sub>2</sub><sup>27</sup>. The film growths on COOH- and OH-terminated SAMs resulted in different crystalline orientations along the [100] and [111] directions. We fabricated MOF thin films on weight-detectable sensors modified with the COOH-terminated SAMs by using crystallization solutions of Cu<sub>3</sub>(BTC)<sub>2</sub> and Zn<sub>4</sub>O(BDC)<sub>3</sub>.

The gold electrodes of 9 MHz AT-cut QCMs were functionalized with the SAM monolayer with COOH-terminates. After the formation of the SAM, the QCMs were placed horizontally onto a Teflon plate with a circular window and the gold electrodes were exposed to a clear crystallization solution of Cu<sub>3</sub>(BTC)<sub>2</sub>. While no Cu<sub>3</sub>(BTC)<sub>2</sub> crystals were obtained on the QCMs without the SAM modification, the dense layer of micrometer-sized Cu<sub>3</sub>(BTC)<sub>2</sub> crystals on the COOH-terminated SAM was formed with a uniform orientation (Figure 1a). The FT-IR-RAS spectrum of the Cu<sub>3</sub>(BTC)<sub>2</sub> crystal on the QCM displayed two peaks at 1390 and 1600 cm<sup>-1</sup>, indicating the formation of coordination bonds between the carboxyl groups in the BTC ligand and copper ions<sup>27</sup> (Fig. S1). A thermo-gravimetric analysis (TGA) of the crystals showed the weight losses of -18.5% from 20 to 120 °C (-H<sub>2</sub>O) and -28.4% from 250 to 400 °C (-CO<sub>2</sub> and others)<sup>24</sup> (Fig. S2). The TGA profile is almost coincidence to the reported profile of Cu<sub>3</sub>(BTC)<sub>2</sub>. The x-ray diffraction pattern of the thin Cu<sub>3</sub>(BTC)<sub>2</sub> films on the QCMs indicated only two (200) and (400) reflections, implying the highly oriented crystalline growth

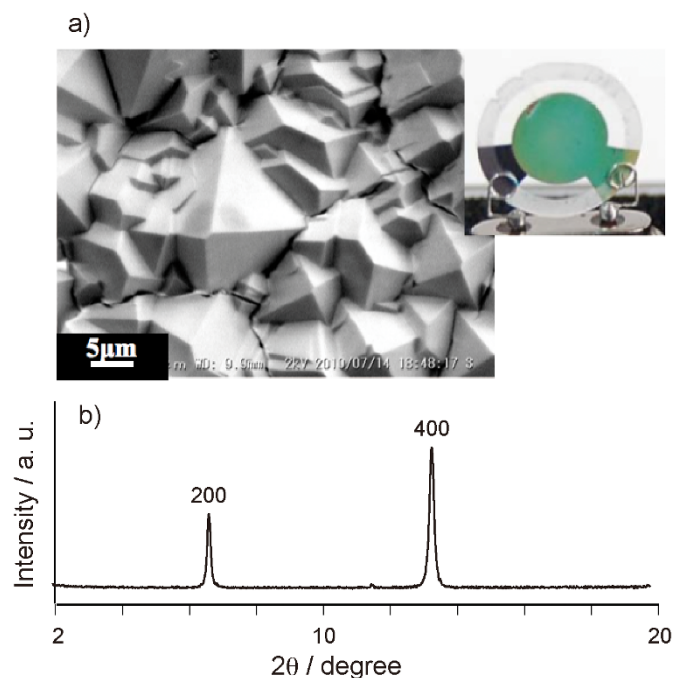
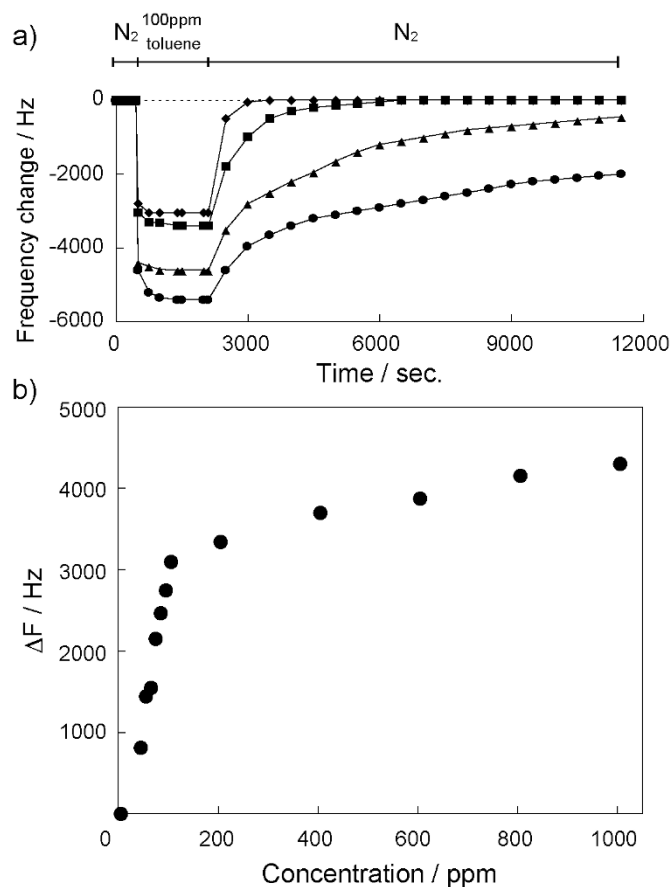


**Figure 1** | a) SEM image and photograph of Cu<sub>3</sub>(BTC)<sub>2</sub> thin film grown from COOH-terminated SAM on gold electrode of QCM. b) Out-of-plane XRD data for Cu<sub>3</sub>(BTC)<sub>2</sub> film on QCM.

along the [100] direction on the COOH-terminated SAM layer (Figure 1b, Fig. S3)<sup>27</sup>. The average film thickness of Cu<sub>3</sub>(BTC)<sub>2</sub> on the QCMs was 500 ± 50 nm estimated from the frequency decrease of the QCMs after the deposition of the crystals, the area of electrode, and the reported density of Cu<sub>3</sub>(BTC)<sub>2</sub>. From these results, highly ordered thin Cu<sub>3</sub>(BTC)<sub>2</sub> films were formed on the QCM sensors modified with the COOH-terminated SAMs.

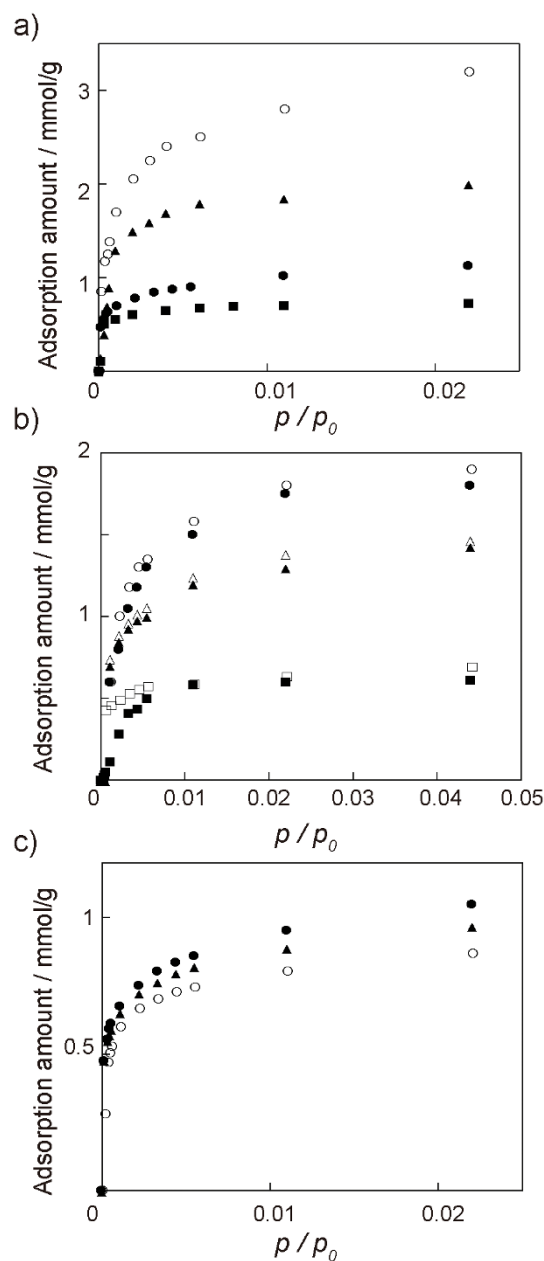
The resonant vibration in a QCM resonator is generated in a direction perpendicular to the surface of the quartz crystal by applying a voltage. The generated vibration propagates within the sensing layer, and the QCMs modified with sensing layers detect the adsorption of analytes by sensing the frequency changes of a resonant vibration. The dissipative loss of the resonance propagation in the sensing layer leads to unstable oscillation due to the contribution of the viscoelastic effect of the sensing layers. The motion resistance of the resonator ( $R_1$ ) in the Butterworth-van Dyke equivalent circuit for the QCMs with Cu<sub>3</sub>(BTC)<sub>2</sub> were investigated using a network impedance analyzer<sup>32</sup>. The motional resistance provides information on the dissipative losses for the resonance propagation of the films on the QCMs. The  $R_1$  value of a Cu<sub>3</sub>(BTC)<sub>2</sub>-coated QCM was almost constant at about 10 Ω within a temperature range of 0–100 °C, indicating there was a small dissipative loss in the Cu<sub>3</sub>(BTC)<sub>2</sub> layer on the QCM (Fig. S4). The QCMs with stiff Cu<sub>3</sub>(BTC)<sub>2</sub> layers exhibited a stable oscillation through the good resonance propagation within this temperature range.

The QCMs modified with Cu<sub>3</sub>(BTC)<sub>2</sub> were set into the temperature-controlled measurement chamber, and the sensing properties were investigated by measuring the frequency changes when the film was exposed to VOC vapors in the chamber<sup>11</sup>. During the exposure phase, the adsorption of the VOC molecules within the MOF layer causes the frequency to decrease. After reaching a constant frequency, the incorporated VOC molecules are released by the supply of pure nitrogen carrier gas. During the desorption process, the frequency of the sensors rises due to the mass decrease in the MOF layer. The frequency changes can be converted into weight changes by using the Sauerbrey equation<sup>33</sup>.



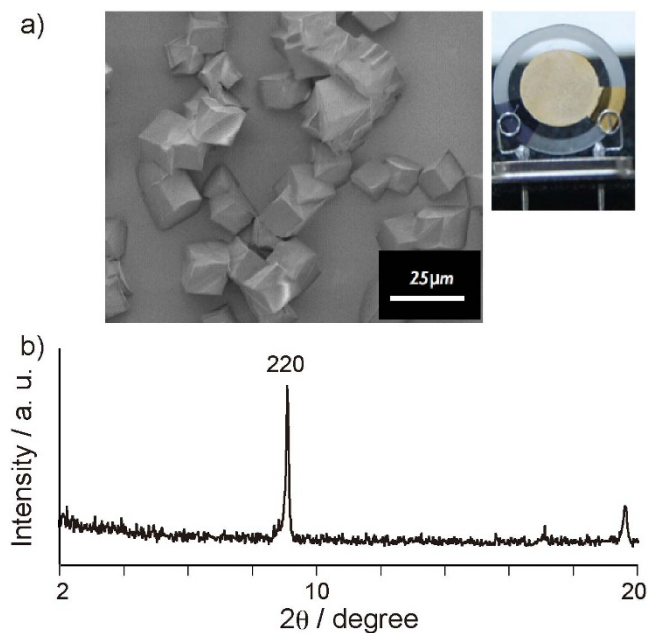
**Figure 2** | a) Responses of QCM sensors modified with  $\text{Cu}_3(\text{BTC})_2$  exposure to 100 ppm toluene vapor at 20 (●), 30 (▲), 40 (■), and 60°C (◆). Dotted line is a response of QCM sensor without  $\text{Cu}_3(\text{BTC})_2$  exposure to 100 ppm toluene vapor at 60°C. b) Frequency change versus toluene concentration at 60°C.

Figure 2a shows the time course of the sensor responses ( $\Delta F$ ) of the QCMs coated with  $\text{Cu}_3(\text{BTC})_2$  responding to exposure to a 100 ppm toluene vapor at 20, 30, 40 and 60°C. The frequency of the QCM operated at 60°C rapidly decreased in response to the toluene vapor exposure, and the signal stayed constant at  $-\Delta F = 3000$  Hz after equilibrium was achieved. When the carrier gas changed to pure nitrogen gas, the frequency returned to the initial state within 5 min, which indicates reversible adsorption/desorption processes of toluene. The sensor exhibited a good repeatability for toluene sensing (Fig. S5). Although the maximum responses for a 100 ppm toluene vapor increased with decreasing operation temperature, the desorption process was slower than that at 60°C. The concentration-dependent responses to the toluene vapor are shown in Figure 2b. The response appeared to increase linearly in the concentration range of 0–100 ppm and saturated above 100 ppm, which was followed by the Langmuir sorption model based on the presence of a set number of nanopores within the  $\text{Cu}_3(\text{BTC})_2$  layer. A concentration increase of 10 ppm in toluene vapor causes a frequency shift of 90 Hz for the QCM sensor with the  $\text{Cu}_3(\text{BTC})_2$  layer. The detection limit for the QCM sensor with the  $\text{Cu}_3(\text{BTC})_2$  layer was evaluated by a concentration change leading to a signal meeting the signal-to-noise ratio conventions of the IUPAC (S/N: 3/1)<sup>34</sup>. We found that the detection limit for toluene was about 1 ppm (a noise level is  $\pm 1.5$  Hz). This detection limit for the  $\text{Cu}_3(\text{BTC})_2$  layer is good compared to our previously reported values for polymer and nanoparticle-based sensing layers<sup>8–11</sup>, suggesting that the porous MOF layers play an effective concentrator for the VOC vapors on weight-detectable sensors.



**Figure 3** | a) Vapor response isotherms of QCM sensors modified with  $\text{Cu}_3(\text{BTC})_2$  to ethanol (○), acetone (▲), toluene (●), and n-octane (■) at 60°C. b) Vapor response isotherms to n-hexane (○), n-hexanol (●), n-heptane (Δ), n-heptanol (▲), n-octane (□), and n-octanol (■) at 60°C. (c) Vapor response isotherms to *o*-xylene (●), *m*-xylene (▲), and *p*-xylene (○) at 60°C.

Figure 3a shows the adsorption isotherms of QCMs coated with  $\text{Cu}_3(\text{BTC})_2$  for four VOCs recorded at 60°C. The  $\text{Cu}_3(\text{BTC})_2$ -coated QCM isotherms for four VOCs showed a Langmuir-type sorption within this concentration range, and the response sequence was ethanol > acetone > toluene > n-octane. The selectivity of the VOC sensing is caused by the following two factors, the chemical interactions of the VOCs with the MOF internal surface and the molecular sieving effect of the regulated nanospace within the three-dimensional MOF frameworks. Since the internal surface of  $\text{Cu}_3(\text{BTC})_2$  is hydrophilic due to the presence of two water molecules coordinated at the axial positions of the  $\text{Cu}^{2+}$ -paddlewheels, the hydrophilic surface can interact with any polar VOC vapors such as ethanol and acetone. The regulated pore and aperture sizes in the



**Figure 4** | a) SEM image and photograph of  $\text{Zn}_4\text{O}(\text{BDC})_3$  thin film grown from COOH-terminated SAM on gold electrode of QCM. b) Out-of-plane XRD data for  $\text{Zn}_4\text{O}(\text{BDC})_3$  film on QCM.

crystalline MOFs would allow for the size selectivity of the adsorption process of the VOCs. Figure 3b shows the adsorption isotherms of  $\text{Cu}_3(\text{BTC})_2$ -coated QCMs for alkanes and alkyl alcohols possessing different alkyl chain lengths. The isotherm of *n*-hexanol was almost consistent with that of *n*-hexane, and the response sequence followed the molecular size of the VOCs. Furthermore, the sensors displayed different isotherms for *o*-xylene, *m*-xylene, and *p*-xylene, implying the recognition of positional isomers of xylene compounds by the  $\text{Cu}_3(\text{BTC})_2$  layer (Figure 3c). Thus, the  $\text{Cu}_3(\text{BTC})_2$  layer provides for the selectivity of VOC sensing to the weight-detectable sensors through the size-selective adsorption of the VOCs within the regulated nanospace of the MOFs.

A thin film of  $\text{Zn}_4\text{O}(\text{BDC})_3$  was also grown from the COOH-terminated SAM onto the gold electrodes of the QCMs by using the crystallization solution. Highly-ordered thin  $\text{Zn}_4\text{O}(\text{BDC})_3$  films were formed on the SAMs as confirmed by SEM and X-ray diffraction pattern (Figure 4a and b).  $\text{Zn}_4\text{O}(\text{BDC})_3$  possesses larger pore size (0.8 nm) and aperture sizes (1.2 and 1.5 nm) than  $\text{Cu}_3(\text{BTC})_2$  due to a network of zinc oxide tetrahedrals connected with the BTC linkers in the highly-crystalline cubic structure (Fig. S6)<sup>25</sup>. Whereas the  $\text{Cu}_3(\text{BTC})_2$  layer showed the difference in the response speeds between the adsorption and desorption processes at 20°C, the reversible responses in both processes were observed in the  $\text{Zn}_4\text{O}(\text{BDC})_3$ -coated QCMs at 20°C (Figure 5a). The sensitivity of the  $\text{Zn}_4\text{O}(\text{BDC})_3$ -coated QCMs was slightly lower than that of the sensor coated with  $\text{Cu}_3(\text{BTC})_2$  as determined from the slopes of the concentration-dependent responses to the toluene vapor (Figure 5b). While the response sequence of the  $\text{Zn}_4\text{O}(\text{BDC})_3$  layer is the same as that of the  $\text{Cu}_3(\text{BTC})_2$  layer, the selectivity of the  $\text{Zn}_4\text{O}(\text{BDC})_3$  layer for the VOCs was lower compared to the  $\text{Cu}_3(\text{BTC})_2$  layer (Figure 5c). The larger pore and aperture sizes in  $\text{Zn}_4\text{O}(\text{BDC})_3$  induced a low molecular sieving effect for the selective sorption of the VOCs. When two MOF thin films were used as the sensing layers of the sensor arrays, the combination of different responses from the two MOF films enables for the detection of the VOC species as well as the determination of the VOC concentration.

Allendorf et al. demonstrated effective sensing of water and alcohols by using microcantilever modified with a MOF thin film<sup>22</sup>. The adsorption and desorption of the vapors in the MOFs on the can-

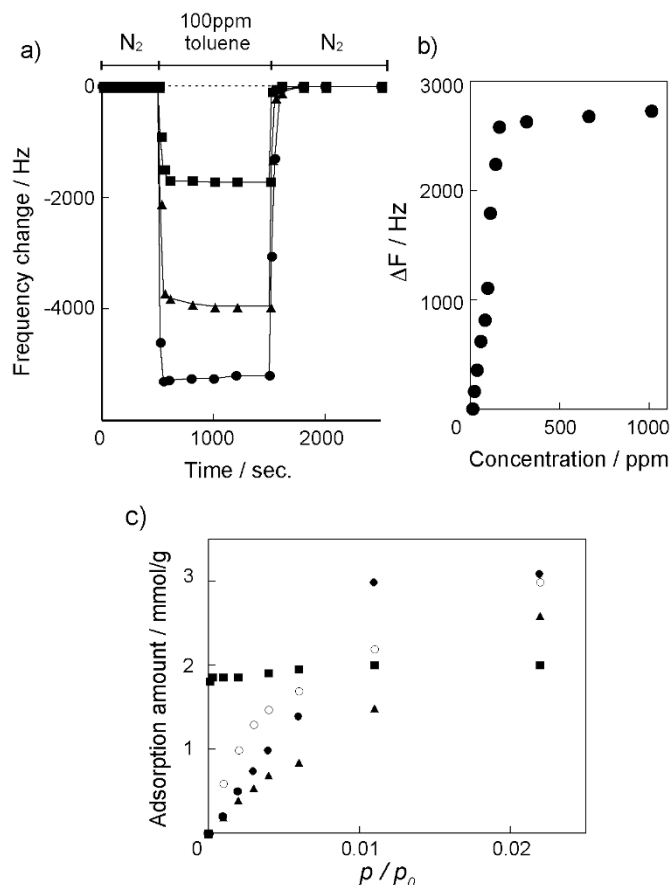


**Figure 5** | a) Responses of QCM sensors modified with  $\text{Zn}_4\text{O}(\text{BDC})_3$  exposure to 100 ppm toluene vapor at 20 (●), 40 (▲), and 60°C (■). Dotted line is a response of QCM sensor without  $\text{Zn}_4\text{O}(\text{BDC})_3$  exposure to 100 ppm toluene vapor at 60°C. b) Frequency change versus toluene concentration at 60°C. c) Vapor response isotherms of QCM sensors modified with  $\text{Zn}_4\text{O}(\text{BDC})_3$  to ethanol (○), acetone (▲), toluene (●), and *n*-octane (■) at 60°C.

tilver produce strain changes at the interface between the MOF film and the cantilever surface. The resultant stress induces the bending of the cantilever and is detected by a piezoresistive sensor on the microcantilever. We also demonstrated the detection of VOCs by monitoring the oscillation frequency and resistance changes of silicon microcantilever sensor chips coated with  $\text{TiO}_2$  porous films covered with polythiophene layers<sup>11</sup>. The oscillation frequency changes were electrically detected by a set of four-bridged piezoresistive gauges on the sensor chip<sup>35,36</sup>. The MOF thin films grown on the microcantilevers can be used to detect VOCs at ppm concentrations.  $\text{Cu}_3(\text{BTC})_2$  crystals were deposited onto the surface of the cantilevers (Figure 6a). A sensor chip with eight cantilevers coated with  $\text{Cu}_3(\text{BTC})_2$  was set into a temperature-controlled chamber, and the sensing properties were investigated by measuring the frequency changes when the film was exposed to VOC vapors in the chamber (Fig. S7). Figure 6b shows the responses of a  $\text{Cu}_3(\text{BTC})_2$ -coated microcantilever sensor to 100 ppm VOC vapors operated at 60°C. The resonant frequency changed according to the adsorption and desorption processes of the VOC vapors on the surface of the  $\text{Cu}_3(\text{BTC})_2$  layer, and the  $\text{Cu}_3(\text{BTC})_2$  layer on the cantilever displayed an effective selectivity for the VOCs. The frequency rapidly decreased in response to the 100 ppm toluene vapor exposure, and the signal stayed constant at  $-\Delta F = 360$  Hz. The integration of MOF thin films with a microcantilever sensor platform can detect VOCs through the analyses of the oscillation frequency as a result of the adsorption/desorption of VOCs within the MOFs.

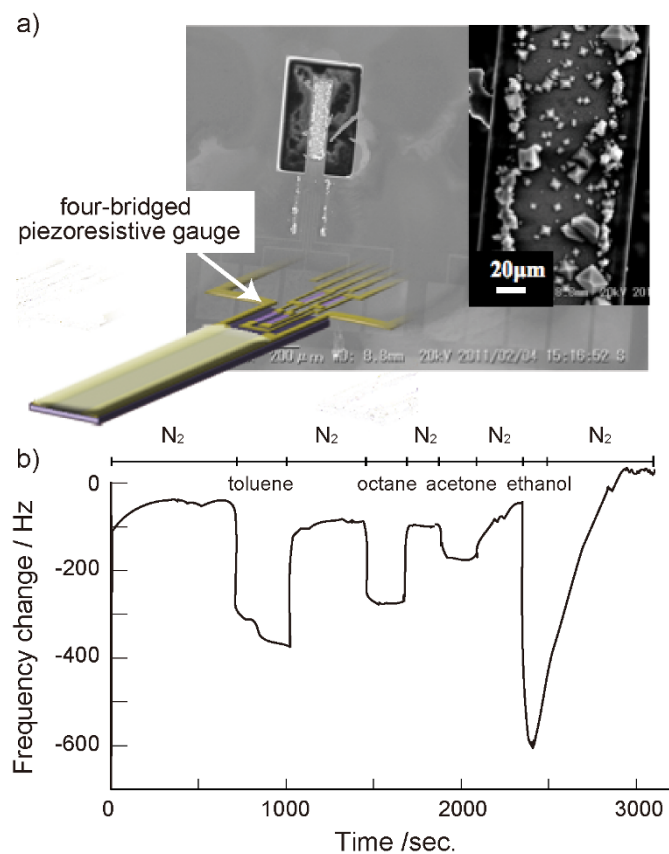


**Figure 6** | a) SEM images of  $\text{Cu}_3(\text{BTC})_2$  thin film grown from COOH-terminated SAM on gold electrode of microcantilever resonator. b) Frequency response of  $\text{Cu}_3(\text{BTC})_2$  film on the microcantilever resonator upon exposure to 100 ppm toluene, n-octane, acetone, and ethanol vapors.

## Discussion

We have demonstrated the detection of VOCs by measuring the frequency changes in the weight-detectable sensors modified with porous MOF layers. The large surface area and regulated nanospace of the MOF layers enhanced their sensitivity and selectivity for VOC sensing. A QCM coated with a  $\text{Cu}_3(\text{BTC})_2$  layer could detect toluene vapors at a concentration of 1 ppm, and showed different responses to a variety of VOC vapors through the molecular sieving effect of MOFs. Two sensors with  $\text{Cu}_3(\text{BTC})_2$  and  $\text{Zn}_4\text{O}(\text{BDC})_3$  provided different sensitivities for VOCs. The tunability of the pore and aperture sizes in the MOFs is an advantage for the creation of a pattern recognition library of chemical sensor arrays for electronic nose systems. Weight-detectable sensors coated with MOFs are a promising sensing platform to realize electronic nose systems. Work is underway to fabricate electronic nose systems for the on-site and real-time analyses of VOCs in ambient environments<sup>37</sup>. On-site and real-time analyses of trace VOCs allow us to provide situational awareness for managing the surrounding hazards. The detection of the VOCs generating from our bodies will open up a new possibility for non-invasive and fast health monitoring, such as for cancer, kidney diseases and neurodegenerative diseases<sup>38–41</sup>.

## Methods

**Chemical Sensing of VOCs by modified QCM and Microcantilever Sensors.** QCM sensors (TamaDevice Co., Ltd., diameter of gold electrode: 5.0 mm) consists of a disk-shaped AT-cut piezoelectric quartz crystal deposited with gold electrodes on both sides, and are operated at a frequency of 9 MHz. Microcantilever arrays have been fabricated according to the previously reported procedures from single crystal silicon (a dimension of cantilever: 100  $\mu\text{m}$  width, 500  $\mu\text{m}$  length, and 5  $\mu\text{m}$  thickness)<sup>35,36</sup>. The deflection of the cantilevers detected electrically by a set of four-bridged

piezoresistive gauges (PGs) and two gold electrodes with a 30  $\mu\text{m}$  distance were deposited on top surface of the cantilevers. The single sensor chip (5 mm  $\times$  5 mm) including eight cantilevers was glued on a lead zirconate titanate (PZT) plate of 0.5  $\mu\text{m}$  thick using silver paste to give vibration, and these units were mounted on a 48-pin quad flat ceramic package. The PGs and PZT plate were electrically connected by gold bonding wires (wire diameter is 25  $\mu\text{m}$ ) to the package leads. The cantilever was driven at around 420 KHz by the use of feedback oscillation circuit for self-oscillation, which was comprised of signal amplifier, phase controller, band pass filter, and automatic gain controller. This circuit allows us selective oscillation of higher vibration modes of the cantilever by adjusting the band pass filter.

The surface of QCMs and microcantilevers were cleaned by the treatment with  $\text{O}_3$ . The cleaned gold electrodes were modified with monolayer of  $\text{HS}(\text{CH}_2)_{15}\text{COOH}$  by immersing into a ethanol solution (30 ml) of NanoThinks™ ACID16 (Aldrich, 0.1 ml), and stand for 48 hr at room temperature. The surface modified sensors were repeatedly washed with ethanol and stored in ethanol.

The crystallization solution of  $\text{Cu}_3(\text{BTC})_2$  was prepared according to the reported method<sup>27</sup>. The SAM-modified QCMs and microcantilevers were held horizontally onto Teflon plate having a window and the gold electrodes were exposed to a clear crystallization solution of  $\text{Cu}_3(\text{BTC})_2$  (Scheme S1). The Teflon plate was placed in a glass petri dish containing 5 ml dimethyl sulfoxide (DMSO) and the vessel was sealed at 123 °C for 6 hr. After 6 hr, the sensors with  $\text{Cu}_3(\text{BTC})_2$  were washed with  $\text{CHCl}_3$  and dried for 3 hr at 150 °C.

The crystallization solution of  $\text{Zn}_4\text{O}(\text{BDC})_3$  was prepared by the following procedure.  $\text{Zn}(\text{NO}_3)_2 \cdot 6\text{H}_2\text{O}$  (78 mg, 0.26 mmol) was added to a 5 ml *N,N*-diethylformamide solution of terephthalic acid (17.5 mg, 0.10 mmol) in sealed glass reactor, and left for 72 hr at 75 °C. After 72 hr, the crystals were removed by filtration and obtained a clear crystallization solution of  $\text{Zn}_4\text{O}(\text{BDC})_3$ .  $\text{Zn}_4\text{O}(\text{BDC})_3$  crystals were grown on the SAM-modified gold electrodes by the contact with crystallization solution for 8 hr at 60 °C. The sensors with  $\text{Zn}_4\text{O}(\text{BDC})_3$  were washed with  $\text{CHCl}_3$  and dried for 3 hr at 150 °C.

VOC sensitivities of the sensing layers on QCM, microelectrode, and microcantilever sensors were investigated using a temperature-controlled chamber designed for measuring simultaneously frequency change. Test vapors were generated by the gas calibration unit using ultra-pure nitrogen gas as a carrier gas. Diluted gases are led into the measuring chamber by the computer-driven magnetic valve systems<sup>41</sup>. The frequency changes of sensors were monitored in response to the incorporation of VOCs. Temperature in the measuring chamber was stabilized by a Peltier thermostat to avoid the temperature-dependent frequency changes, and temperature of the chamber was monitored during the experiments. Six universal frequency counters (Agilent Technology, Model 53131A) are able to determine twelve frequencies at the same time. For each test gas, five repeated frequency changes were analyzed for the variation of  $-\Delta F$  to determine reproducibility. The standard deviation in the frequency changes was less than the noise level of QCMs ( $\pm 1.5$  Hz).

- Pearce, T. C., Schiffman, S. S., Nagle, H. T. & Gardner, J. W. *Handbook of Machine Olfaction Electronic Nose Technology* (Wiley-VCH, Weinheim, 2003).
- Röck, F., Barsan, N. & Weimar, U. Electronic Nose: Current Status and Future Trends. *Chem. Rev.* **108**, 705–725 (2008).
- Nakamoto, T. *Human Olfactory Displays and Interfaces: Odor Sensing and Presentation* (Information Science Reference, Hershey, PA, 2012).
- Potyrailo, R. A. & Mirsky, V. M. Combinatorial and High-Throughput Development of Sensing Materials: The First 10 Years. *Chem. Rev.* **108**, 771–813 (2008).
- Miller, T. A., Bakrania, S. D., Perez, C. & Wooldridge, M. S. [Nanostructured Tin Oxide Materials for Gas Sensor Applications]. *Functional Nanomaterials* [Geckeler, K. E. & Rosenberg, E. (ed.)] [1–24] (American Scientific Publishers, 2006).
- Janshoff, A., Galla, H. -J. & Steinem, C. Piezoelectric Mass-Sensing Devices as Biosensors –An Alternative to Optical Biosensors? *Angew. Chem. Int. Ed.* **39**, 4004–4032 (2000).
- Goeders, K. M., Colton, J. S. & Bottomley, L. A. Microcantilevers: Sensing Chemical Interactions via Mechanical Motion. *Chem. Rev.* **108**, 522–542 (2008).
- Kimura, M., Sugawara, M., Sato, S., Fukawa, T. & Mihara, T. Volatile Organic Compounds Sensing by Quartz Crystal Microbalance Coated with Nanostructured Macromolecular Metal Complexes. *Chem. Asian J.* **5**, 869–876 (2010).
- Kimura, M. *et al.* Detection of Volatile Organic Compounds by Analyses of Polymer-coated Quartz Crystal Microbalance Sensor Arrays. *Sensor Mater.* **23**, 359–368 (2011).
- Kimura, M., Yokokawa, M., Sato, S., Fukawa, T. & Mihara, T. VOC Sensing by Gold Nanoparticles Capped with Calix[4]arene Ligands. *Chem. Lett.* **40**, 1402–1404 (2011).
- Kimura, M. *et al.* Sensing of Vaporous Organic Compounds by  $\text{TiO}_2$  Porous Films Covered with Polythiophene Layers. *Adv. Funct. Mater.* **22**, 469–476 (2012).
- Yaghi, O. M. *et al.* Reticular synthesis and the design of new materials. *Nature* **423**, 705–714 (2003).
- Kitagawa, S., Kitaura, R. & Noro, S. Functional Porous Coordination Polymers. *Angew. Chem. Int. Ed.* **43**, 2334–2375 (2004).
- Mueller, U. *et al.* Metal-organic frameworks-perspective industrial applications. *J. Mater. Chem.* **16**, 626–636.



15. Lee, J. Y. *et al.* Metal-organic frameworks materials as catalysts. *Chem. Soc. Rev.* **38**, 1450–1459 (2009).
16. Zhao, X. *et al.* Hysteretic Adsorption and Desorption of Hydrogen by Nanoporous Metal-Organic Frameworks. *Science* **306**, 1012–1015 (2004).
17. Wang, C., Liu, D. & Lin, W. Metal-Organic Frameworks as A Tunable Platform for Designing Functional Molecular Materials. *J. Am. Chem. Soc.* **135**, 13222–13234 (2013).
18. Kreno, J. E. *et al.* Metal-Organic Framework Materials as Chemical Sensors. *Chem. Rev.* **112**, 1105–1125 (2012).
19. Ameloot, R. *et al.* Patterned Growth of Metal-Organic Framework Coating by Electrochemical Synthesis. *Chem. Mater.* **21**, 2580–2582 (2009).
20. Kreno, L. E., Hupp, J. T. & Van Duyne, R. P. Metal-Organic Framework Thin Film for Enhanced Localized Surface Plasmon Resonance Gas Sensing. *Anal. Chem.* **82**, 8042–8046 (2010).
21. Biemmi, E., Draga, A., Stock, N. & Bein, T. Direct growth of  $\text{Cu}_3(\text{BTC})_2(\text{H}_2\text{O})_3 \cdot x\text{H}_2\text{O}$  thin films on modified QCM-gold electrodes – Water sorption isotherms. *Micropor. Mesopor. Mat.* **114**, 380–386 (2008).
22. Allendorf, M. D. *et al.* Stress-Induced Chemical Detection Using Flexible Metal-Organic Frameworks. *J. Am. Chem. Soc.* **130**, 14404–14405 (2008).
23. Robinson, A. L. *et al.* Ultrasensitive Humidity Detection Using Metal-Organic Framework-Coated Microsensors. *Anal. Chem.* **84**, 7043–7051 (2012).
24. Chui, S. S. -Y., Lo, S. M. -F., Charmant, J. P. H., Orpen, A. G. & Williams, I. D. A Chemically Functionalizable Nanoporous Materials  $[\text{Cu}_3(\text{TMA})_2(\text{H}_2\text{O})_3]_n$ . *Science* **283**, 1148–1150 (1999).
25. Rosi, N. L. *et al.*, Hydrogen Storage in Microporous Metal-Organic Frameworks. *Science* **300**, 1127–1129 (2003).
26. Shekhah, O. *et al.* Step-by-Step Route for the Synthesis of Metal-Organic Frameworks. *J. Am. Chem. Soc.* **129**, 15118–15119 (2007).
27. Biemmi, E., Scherb, C. & Bein, T. Oriented Growth of the Metal Organic Framework  $\text{Cu}_3(\text{BTC})_2(\text{H}_2\text{O})_3 \cdot x\text{H}_2\text{O}$  Tunable with Functionalized Self-Assembled Monolayers. *J. Am. Chem. Soc.* **129**, 8054–8055 (2007).
28. Carbonell, C., Imaz, I. & Maspoch, D. Single-Crystal Metal-Organic Framework Arrays. *J. Am. Chem. Soc.* **133**, 2144–2147 (2011).
29. Otsubo, K. *et al.* Step-by-Step Fabrication of a Highly Oriented Crystalline Three-Dimensional Pillared-Layer-Type Metal-Organic Framework Thin Films Confirmed by Synchrotron X-ray Diffraction. *J. Am. Chem. Soc.* **134**, 9605–9608 (2012).
30. Xu, G., Yamada, T., Otsubo, K., Sakaida, S. & Kitagawa, H. Facile “Molecular Assembly” for Fast Construction of a Highly Oriented Crystalline MOF Nanofilm. *J. Am. Chem. Soc.* **134**, 16524–16527 (2012).
31. Stavila, V., Volponi, J., Katzenmeyer, A. M., Dixon, M. C. & Allendorf, M. D. Kinetics and mechanism of metal-organic framework thin film growth: systematic investigation of HKUST-1 deposition on QCM electrodes. *Chem. Sci.* **3**, 1531–1540 (2012).
32. Grate, J. W., Nelson, D. A. & Skaggs, R. Sorptive Behavior of Monolayer-Protected Gold Nanoparticle Films: Implication for Chemical Vapor Sensing. *Anal. Chem.* **75**, 1868–1879 (2003).
33. Sauerbrey, G. Verwendung von Schwingquarzen zur Wägung dünner Schichten und zur Mikrowägung. *Zeitschrift für Physik* **155**, 206–222 (1959).
34. Dickert, F. L., Forth, P., Lieberzeit, P. & Tortschanoff, M. Molecular imprinting in chemical sensing – Detection of aromatic and halogenated hydrocarbons as well as polar solvent vapors. *Fresenius J. Anal. Chem.* **360**, 759–762 (1998).
35. Ikehara, T., Lu, J., Konno, M., Maeda, R. & Mihara, T. A high quality-factor silicon cantilever for a low detection-limit resonant mass sensor operated in air. *J. Micromech. Microeng.* **17**, 2491–2494 (2007).
36. Ikehara, T. *et al.* Integration of p-n Junction Diode to Cantilever Mass Sensors for Frequency Drift Compensation due to temperature Fluctuation. *Sensor Mater.* **23**, 381–396 (2011).
37. Mihara, T. *et al.* Design, Fabrication, and Evaluation of Highly Sensitive Compact Chemical Sensor System Employing a Microcantilever Array and a Preconcentrator. *Sensor Mater.* **23**, 397–417.
38. Hakim, M. *et al.* Volatile Organic Compounds of Lung Cancer and Possible Biochemical Pathways. *Chem. Rev.* **112**, 5949–5966 (2012).
39. Peng, G. *et al.* Diagnosing lung cancer in exhaled breath using gold nanoparticles. *Nat. Nanotech.* **4**, 669–673 (2009).
40. Konvalina, G. & Haick, H. Sensors for Breath Testing: From Nanomaterials to Comprehensive Disease Detection. *Acc. Chem. Res.* **47**, 66–76 (2014).
41. Braza, Y. Y., Zuri, L. & Haick, H. Combined Volatolomics for Monitoring of Human Body Chemistry. *Sci. Rep.* **4**, 4611 (2014).

## Acknowledgments

This work was partially supported by “Regional Innovation Cluster Program of Nagano” from the Ministry of Education, Culture, Sports, Science, and Technology, Japan.

## Author contributions

T.M. conceived the original idea and guided the project. M.K. designed sensing materials and wrote the manuscript. H.Y., S.S. and T.F. carried out material characterization and sensing measurements. T.I. and R.M. carried out design and fabrication of silicon-based microcantilevers. All authors assisted with the manuscript preparation and discussed the results.

## Additional information

Supplementary information accompanies this paper at <http://www.nature.com/scientificreports>

**Competing financial interests:** The authors declare no competing financial interests.

**How to cite this article:** Yamagiwa, H. *et al.* Detection of Volatile Organic Compounds by Weight-Detectable Sensors coated with Metal-Organic Frameworks. *Sci. Rep.* **4**, 6247; DOI:10.1038/srep06247 (2014).



This work is licensed under a Creative Commons Attribution 4.0 International License. The images or other third party material in this article are included in the article's Creative Commons license, unless indicated otherwise in the credit line; if the material is not included under the Creative Commons license, users will need to obtain permission from the license holder in order to reproduce the material. To view a copy of this license, visit <http://creativecommons.org/licenses/by/4.0/>